Tree Physiology 39, 1300–1312
doi:10.1093/treephys/tpz062

Research paper

Plant water content integrates hydraulics and carbon depletion to predict drought-induced seedling mortality

Gerard Sapes[1,7], Beth Roskilly[1], Solomon Dobrowski[2], Marco Maneta[3], William R. L. Anderegg[4], Jordi Martinez-Vilalta[5,6] and Anna Sala[1]

[1]Division of Biological Sciences, University of Montana, Missoula, MT 59812, USA; [2]Department of Forest Management, University of Montana, Missoula, MT 59812, USA; [3]Department of Geosciences, University of Montana, Missoula, MT 59812, USA; [4]School of Biological Sciences, University of Utah, Salt Lake City, UT 84103, USA; [5]Centre de Recerca Ecològica i Aplicacions Forestals (CREAF) Cerdanyola del Vallès 08193 Barcelona, Spain; [6]Universitat Autònoma de Barcelona, Cerdanyola del Vallès 08193 Barcelona, Spain; [7]Corresponding author (gsapes@umn.edu) orcid.org/0000-0002-6017-2053, orcid.org/0000-0002-6017-2053

Received January 28, 2019; accepted May 13, 2019; handling Editor Danielle Way

Widespread drought-induced forest mortality (DIM) is expected to increase with climate change and drought, and is expected to have major impacts on carbon and water cycles. For large-scale assessment and management, it is critical to identify variables that integrate the physiological mechanisms of DIM and signal risk of DIM. We tested whether plant water content, a variable that can be remotely sensed at large scales, is a useful indicator of DIM risk at the population level. We subjected *Pinus ponderosa* Douglas ex C. Lawson seedlings to experimental drought using a point of no return experimental design. Periodically during the drought, independent sets of seedlings were sampled to measure physiological state (volumetric water content (VWC), percent loss of conductivity (PLC) and non-structural carbohydrates) and to estimate population-level probability of mortality through re-watering. We show that plant VWC is a good predictor of population-level DIM risk and exhibits a threshold-type response that distinguishes plants at no risk from those at increasing risk of mortality. We also show that plant VWC integrates the mechanisms involved in individual tree death: hydraulic failure (PLC), carbon depletion across organs and their interaction. Our results are promising for landscape-level monitoring of DIM risk.

Keywords: carbon starvation, drought, hydraulic failure, non-structural carbohydrates, *Pinus ponderosa*.

Introduction

Climate change is expected to increase the frequency and intensity of drought (Stocker et al. 2015), which in turn will lead to increases of drought-induced forest mortality (DIM) (Lewis et al. 2011, Williams et al. 2013, Allen et al. 2015, Rowland et al. 2015, Stocker et al. 2015). In addition to social and economic consequences, DIM can also have profound consequences for global water and carbon cycles and vegetation–climate feedbacks. Thus, to accurately monitor and manage DIM, we must identify reliable plant variables that provide early warning signals of DIM risk, integrate physiological mechanisms driving DIM and that can be measured at large spatial scales (Hartmann et al. 2018). During the past decade, research has identified hydraulic failure (i.e., loss of water transport in the xylem) as a dominant physiological mechanism of DIM, with non-structural carbohydrate (NSC) depletion often playing a significant interacting role (Adams et al. 2017). Hydraulic failure kills plants when they lose hydraulic conductivity, measured as percent loss of conductivity (PLC), and can no longer supply enough water to living tissues. However, monitoring PLC at the population or stand level is methodologically challenging, which hinders our ability to monitor mortality risk at larger scales. Here, we test whether plant water content, a variable that can be measured remotely (Ceccato et al. 2001, Ullah et al. 2012, Konings et al. 2016), integrates hydraulic failure and carbon depletion mechanisms and is a useful indicator of DIM risk at the

population level (defined as the proportion of dead individuals in a given population or stand at a given point in time).

Regardless of the mechanisms involved, drought kills plants due to progressive dehydration leading to irreversible loss of turgor (Tyree et al. 2003), when living cells lose function. How living plant cells sense dehydration is still under debate (Sack et al. 2018), but it involves changes in cell volume, cell turgor and osmolyte concentration (Zhu 2016, Sack et al. 2018). In most plants, dehydration eventually leads to membrane dysfunction (Wang et al. 2008, Chaturvedi et al. 2014) and death (Guadagno et al. 2017). To avoid death, therefore, plants must retain a minimum pool of water necessary to prevent permanent turgor loss. Under drought, when stomata close and water is lost through cuticles, plant water pools depend on both (i) the ability of the xylem to maintain the supply of water and (ii) the ability of living cells to retain such water by preventing water loss to the xylem and the atmosphere. Under drought and limited soil water availability, emboli form in the xylem and can increase PLC to values leading to hydraulic failure (Tyree and Sperry 1989). Water retention in living cells depends on their ability to decrease cell water potential (WP) to match that of the adjacent xylem, which occurs by concentrating solutes. As NSCs are a source of organic solutes and energy for active transport, NSC depletion could lead to loss of cell water retention and permanent turgor loss via reductions of organic solutes and their osmotic or energetic roles (Brodersen et al. 2010, Sevanto et al. 2014). We propose that reductions in plant water content reflect mortality risk under drought (progressive dehydration) due to the combined effect of hydraulic failure and carbon depletion (Figure 1; Martínez-Vilalta et al. 2019).

Several things support the use of water content as an early warning indicator of drought mortality risk. First, while hydraulic failure appears to be the dominant mechanism of drought mortality, NSC depletion is also thought to play a role (Adams et al. 2017), and the two mechanisms often interact (McDowell 2011, Sala et al. 2012, Meir et al. 2015). However, the nature of this interaction is not well understood and is difficult to model (Mencuccini et al. 2015). A water supply retention approach (Figure 1) under drought mechanistically captures this interaction and integrates it into a single variable: water content. Second, and critical for an indicator variable, just as irreversible turgor loss shows a threshold response, water content is also likely to mirror such a threshold response. Although plants can recover from temporary turgor loss, continued decreases of water content below turgor loss eventually reach a critical value at which irreversible turgor loss, plasmolysis and loss of cell function occur (Trueba et al. 2019). Thus, water content is likely to distinguish plants at no risk of DIM from those at risk as drought proceeds (i.e., to detect incipient risk of mortality). Third, and particularly relevant for the purposes of large-scale monitoring, water content can be measured remotely (Ceccato et al. 2001, Ullah et al. 2012, Konings et al. 2016, Rao et al. 2019). In summary, water content may prove a useful indicator of drought mortality risk because it is likely to integrate the mechanisms of drought mortality at the individual level and to show a threshold response that signals incipient risk of mortality that is measurable at multiple scales.

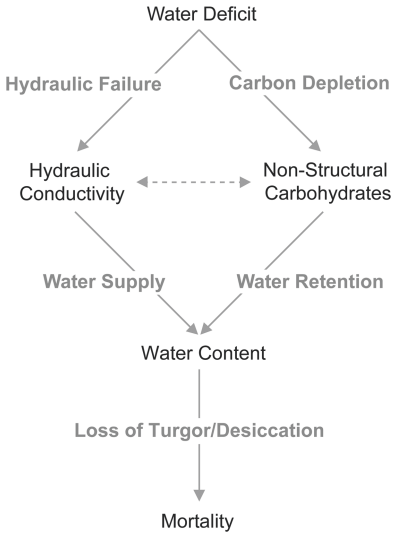

Figure 1. A framework of DIM focused on plant water content. Plants experience dehydration when water supply is insufficient to replace water loss leading to water deficit. Consequently, xylem tension increases leading to embolism formation (hydraulic failure). Likewise, stomatal closure eventually leads to carbon depletion during long periods of drought. Loss of hydraulic function and carbon depletion further limit water supply and retention of tissues leading to inability to maintain water balance, loss of turgor/desiccation and death. Black text indicates variables of interest. Gray text indicates DIM mechanisms. Solid arrows link variables within a given mechanism. Dashed arrows indicate potential (but still controversial) interactions between NSCs and hydraulic conductivity (e.g., embolism repair processes).

Most studies of individual DIM physiological thresholds have focused on measurements of dead or nearly dead plants based on visual cues, including browning, defoliation and branch die-off (Hoffmann et al. 2011, Anderegg et al. 2012*a*, Anderegg and Anderegg 2013, O'Brien et al. 2014, Pratt et al. 2014, Anderegg et al. 2015, Dickman et al. 2015, Rowland et al. 2015, Garcia-Forner et al. 2016, Adams et al. 2017). This approach can be problematic because visual symptoms of plant death generally occur well after plants have crossed the point of no return (the point beyond which plants can no longer survive; Anderegg et al. 2012b), potentially missing early warning physiological signals. Furthermore, for some species, measurements at the leaf or branch level may not be representative of the whole-plant level mortality processes. Thus, fully understanding the processes driving DIM and identifying physiological states that are indicative of DIM risk requires experimental designs based on the point of no return and measurements across all organs. That is, it requires concurrent multi-organ/whole-plant level measurements of potential physiological indicators (PLC, NSC, water content or others such as photosynthesis,

gas exchange and transpiration) at different stages of drought regardless of symptoms and probability of mortality (e.g., by re-watering and subsequent assessment of mortality). As whole-plant measurements are usually destructive, physiological measurements must be independent of mortality assessments. Such an approach entails pairing independent measurements of physiology and probability of mortality to identify the physiological states at which population-level mortality risk increases as drought progresses. These experimental designs are rare (but see Barigah et al. 2013 and Kursar et al. 2009). However, they are highly informative because they can detect incipient mortality thresholds, a critical feature for a monitoring indicator.

We performed a greenhouse drought experiment with 2-year-old ponderosa pine (*Pinus ponderosa* Douglas ex C. Lawson) seedlings to test whether plant water content is a good predictor of DIM risk at the population level. Our experimental design was implemented to detect the point of no return and to focus on potential threshold responses signaling incipient DIM risk. We sampled independent sets of seedlings periodically during the experimental drought to (i) measure their physiological state (e.g., volumetric water content (VWC), PLC and NSC) and (ii) estimate the probability of mortality once re-watered based on their physiological state. We hypothesized that (i) plant water content is related to loss of hydraulic conductivity and NSC availability at both organ and whole-plant levels; (ii) water content is negatively correlated and PLC positively correlated with DIM; and (iii) water content shows a threshold-like response distinguishing healthy plants from those at risk of DIM. We stress that our goal is not to compare the relative performance of water content, PLC or NSC as predictors of DIM, but simply to test whether water content is a useful integrative predictor.

Materials and methods

Study design

The experiment took place at the University of Montana greenhouse facilities. On 2 August 2015 we obtained 250 2-year-old *P. ponderosa* seedlings in soil plugs from the Coeur D'Alene Nursery (USDA Forest Service). Ponderosa pine is one of the most widely distributed species in North America and has been extensively used as a representative of the gymnosperm lineage within ecological, physiological and forestry studies. Seedlings were planted in 7.6 cm diameter × 43 cm tall pots using a homogeneous soil mixture consisting of 3:1:1 sand, peat moss and top soil, respectively. Seedlings ranged from 12.7 to 27.0 cm tall from the base to the tip of the stem with an average height of 20.7 ± 3.1 cm, and soil plugs were ca 20 cm in length. Pots were randomized on a bench at regular distances from each other and left to acclimate for a month under well-watered conditions (i.e., field capacity, when the soil is saturated). Soil field capacity corresponded to soil

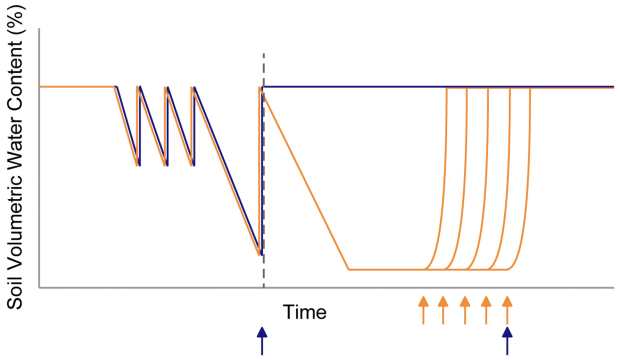

Figure 2. Experimental drought design based on changes in soil VWC_s. All seedlings used for the experiment were drought pre-conditioned in four consecutive dry down cycles. The first three lowered the VWC_s to 50% of field capacity, while the last one to 25% of field capacity. After the last pre-conditioning dry down, five seedlings were kept at field capacity (dark blue) and the rest received no watering (orange). Dark blue represent controls subjected to drought pre-conditioning but kept well-watered through the final dry-down. Orange arrows represent when drought-treated seedlings were measured and the corresponding mortality assessment was conducted (by re-watering a random, independent sample of seedlings). Blue arrows indicate when measurements in control seedlings were done.

VWC_s of ca 20%. Based on preliminary experiments in seven seedlings and for the purpose of timing consecutive samplings, we monitored changes in VWC_s using Decagon 5TE sensors (Decagon Devices, Inc., Pullman, Washington, USA) placed in five representative seedlings 10 cm above the bottom of the pots. Sensors were inserted through a hole drilled on the side of the pots to minimize disturbance and root damage. Roots had reached 40 cm in depth by the end of the experiment.

From 2 September to 1 October, seedlings underwent four drought pre-conditioning cycles to allow plants to acclimate to drought stress. During the first three cycles, we let pots dry down to 50% of their field capacity (VWC_s = 10%) after which we watered again to field capacity. On the last cycle, pots were dried to 25% of their field capacity (VWC_s = 5%), which corresponds to a soil WP of −0.7 MPa based on an empirical soil characteristic curve (see below) and then watered again to field capacity. From 1 October to 1 December, we stopped watering all but 25 seedlings (controls). Drought-treated seedlings were left un-watered for the rest of the experiment, while control seedlings were kept at field capacity (Figure 2). Based on a preliminary drought experiment to assess symptoms of mortality as a function of soil drought and to optimize sampling times and sample size, we started measurements 34 days after the beginning of the drought treatment.

Sampling procedure

We assessed soil WP, seedling physiology and mortality risk on six weekly samplings at Days 0, 34, 41, 48, 55 and 62. At each sampling, we measured midday VWC_s in five randomly chosen seedlings. VWC_s sensors were installed 24 h prior to measurement to reach equilibrium with soil conditions. VWC_s

was then used to estimate the soil WP at which each seedling was exposed to at the time of sampling. To do so, we converted VWC_s values to soil WP based on an empirical soil characteristic curve, describing the relationship between VWC_s and soil WP as a soil dries (Fredlund and Xing 1994). To generate this curve, we dried a pot with the same soil used in the experiment at a constant temperature (ca 40 °C). A VWC_s sensor (Decagon 5TE) and a soil WP sensor (Decagon MPS-6) were placed at the same height in the center of the pot. This process was repeated twice with the same pot to reduce variability due to measurement error.

We also measured leaf WPs. However, these measurements were not reliable because needles became dry and brittle as the drought intensified thus breaking during measurements or becoming hydraulically disconnected from the rest of the plant. We note, however, that this did not prevent us from assessing plant water content, the main goal of this experiment, nor hydraulic failure and carbon depletion, which were measured to assess whether water content integrates these two processes. Also, although plant water status is usually assessed with plant WP, plant water content and PLC also serve as indicators of drought stress. At every sampling date, the same five seedlings in which VWC_s was measured were then harvested and kept in ziplock bags with a moist paper towel in a cooler to prevent further water loss (Garcia-Forner et al. 2016). Samples were transported to the laboratory within 2 h for physiological measurements (see below). Because physiological measurements were destructive, at each sampling event during the drought a second independent subset of randomly sampled seedlings was used to assess mortality risk at the population level (probability of mortality).

Mortality assessment

To estimate the probability of mortality at the population level over time, at each sampling event, 15% of the total pool of drought-treated seedlings (see Table S1 available as Supplementary Data at *Tree Physiology* Online for full range of sample sizes) were randomly chosen, re-watered to field capacity and kept well-watered for at least 39 days (until 8 January) to assess mortality. This method ensures accurate classification of both live and dead plants at every sampling event regardless of visual symptoms. We classified seedlings as dead only if their canopy and phloem were completely brown and dry (Cregg 1994) and no subsequent buds appeared (dead seedlings were left in the greenhouse for two additional months). Notice that early re-watering groups were re-watered for longer periods of time due to the nature of the experimental design. However, seedlings removed at the later stages of the drought were completely dry and brittle with no subsequent signs of recovery. Because the total pool of drought-treated seedlings was reduced every time when mortality probability was assessed, 15% of the total pool of drought-treated seedlings represented a different number of individuals at each sampling event (max: 32; min: 14). To make estimates of mortality comparable across sampling events in terms of sample size, we estimated mortality using only 13 plants randomly subsampled from the pool of plants chosen to estimate mortality at each sampling date. This subsampling procedure was repeated 1000 times using a bootstrapping scheme, and the 1000 values of mortality generated per sampling event were averaged to generate a proxy for population-level probability of mortality at each sampling event (see Table S1 available as Supplementary Data at *Tree Physiology* Online for estimates of the uncertainty around these values). Note that in our design, physiological measurements during drought were done in individual plants and averaged, while mortality measurements were conducted at the population level.

Plant VWC

We separated root systems from the rest of the plant, obtained a stem segment from the base of the stem up to the first needles and collected needles of each seedling. We used these tissues to measure organ VWC based on fresh and dry weights as ((fresh weight − dry weight)/fresh volume)∗100. We measured volume with the water displacement method in a reservoir of deionized water (Olesen 1971, Hughes 2005). Dry weights were measured after hydraulic conductivity measurements (see below). We focused on VWC because this variable can be directly related to variables measured through remote sensing (Yilmaz et al. 2008, Mirzaie et al. 2014, Veysi et al. 2017). We calculated whole plant VWC weighed by organ fraction biomass (proportion of each organ dry mass fraction multiplied by their respective VWC). For consistency, root VWC was measured before any other organ to avoid changes in VWC or hydraulic conductivity due to cleaning procedures and exposure to dry air. After a quick immersion in water to minimize water absorption, we immediately blotted tissues with paper towels until no surface water was left. Stem segments and root systems were returned to ziploc bags and a cooler immediately after measurements of fresh weight and volume, prior to hydraulic conductivity measurements.

Stem and root hydraulics

We measured stem hydraulic conductivity and root hydraulic conductance using the gravimetric method (Sperry et al. 1988) immediately after fresh volume measurements of organs. We used a modification of the hydraulic apparatus described in Sperry et al. (1988) that allowed us to measure hydraulic conductance of whole root systems in addition to stems by measuring the upstream flow of water entering the sample rather than the flow or volume on the downstream end. In our system, a micro-flow sensor (Sensirion SLI-0430, Sensirion, Inc., Staefa ZH, Switzerland) was placed upstream from the stem segment

(instead of a scale) to record water flow. This sensor measures flow every 70 ms with a precision of 1 μL min^{-1}, thus allowing precise measurements in plants with low hydraulic conductivity. Stem segments previously used for VWC measurements were immersed in deionized water for 20 min to relax xylem tensions that could artificially alter conductivity values (Trifilo et al. 2014). After relaxation, stem segments were relocated to the hydraulic apparatus, and each end was re-cut twice at a distance of 1 mm from the tips (total of 2 mm per side) to remove any potential emboli resulting from transport, segment sampling and relocation (Torres-Ruiz et al. 2015). After re-cutting, segments had an average length of 7.03 ± 0.89 cm and ranged from 4.80 to 8.90 cm. Given that plants had an average height of 20.7 cm, the average distance of the end cut of a segment to the top of the stem was 13.67 cm. Stems were then connected to the hydraulic apparatus while under water, with their terminal ends facing downstream flow. The stems were then raised out of the water, and the connections were checked to ensure that there were no leaks.

First, initial background flow was measured to account for the flow existing under no pressure, which can vary depending on the degree of dryness of the measured organ (Hacke et al. 2000, Torres-Ruiz et al. 2012, Blackman et al. 2016). Second, a pressure gradient of 5–8 kPa was applied to run water through the stem and pressurized flow was measured. This small pressure gradient prevented embolism removal from the samples while ensuring flow. Lastly, final background flow was measured, initial and final background flows were averaged and net flow was calculated as the difference between pressurized flow and average background flow. Native specific hydraulic conductivity (K) was estimated in stems as the (net) flow divided by the pressure gradient used and standardized by xylem area and length. Xylem length was measured using a caliper and xylem area was calculated from stem diameter assuming a circular area.

The configuration of the apparatus was then changed to measure whole root system hydraulic conductance using the same gravimetric principle. This approach requires the water to flow backwards through the roots. Such backwards flow has been demonstrated to have no significant effect on hydraulic measurements (Kolb and Robberecht 1996; Tyree et al. 2003). We ensured that both configurations of the apparatus were comparable by measuring stems using both arrangements, and we found no significant differences between them (t = 0.785, P = 0.476). As in stems, roots were also relaxed in deionized water for 20 min to relax xylem tensions that could artificially alter conductivity values (Trifilo et al. 2014). Flow, including initial and final background flow, was measured as above and whole-root native hydraulic conductance (k) was estimated as the (net) flow divided by the pressure gradient used and standardized by xylem area at the root collar.

Maximum stem hydraulic conductivity (Kmax) and root hydraulic conductance ($k$max) were estimated as the average stem K and root k of the well-watered seedlings measured at Day 62 after the onset of the drought and used to calculate PLC in all measured seedlings. Such a population approach was chosen because seedlings were too small to reconnect to the apparatus once cut a second time after removing emboli to measure maximum hydraulic conductivity. Percent loss of stem conductivity and percent loss of root conductance (PLC) were estimated for each measured seedling as $100*(K\text{max} - K)/K\text{max}$ and $100*(k\text{max} - k)/k\text{max}$, respectively. Note that slightly negative PLC values may occur if K or k in a given sample is larger than Kmax estimated as the average K of controls. We evaluate how uncertainty in population-level Kmax can affect PLC values and potential incipient mortality thresholds in Methods S1 available as Supplementary Data at *Tree Physiology* Online. We calculated whole-plant PLC weighted by the proportion of each organ fraction. Root and stem PLC can be averaged together because they are unit-less indexes that represent the relative loss of water transport of their respective organs. Because we did not measure PLC in needles, we defined whole-plant PLC as the overall hydraulic integrity of the stem and root systems only. A solution of water with 10 mM KCl degassed at 3 kPa for at least 8 h was used for all hydraulic measurements (Espino and Schenk 2011). We developed an R code (see Methods S2 available as Supplementary Data at *Tree Physiology* Online) that automatically calculates pressurized and background flows once flow stabilizes. We excluded PLC measurements taken at Days 0 and 34 since the onset of drought (see Figure 3B) because a leakage was detected in our apparatus leading to artificial values. However, this did not prevent us from obtaining PLC values across the full range of observed mortality, including values close to 0 measured at Day 41.

Non-structural carbohydrates

After hydraulic measurements, needle, stem and root samples were microwaved for 180 s at 900 Watts in three cycles of 60 s to stop any metabolic activity. Organs were subsequently oven-dried at 70 °C until constant mass. Samples were weighed and ground to a fine powder. Approximately 11 mg of needle tissue and 13 mg of stem or root tissue were used to analyze NSC dry mass content following the procedures and enzymatic digestion method from Hoch et al. (2002) and Galiano et al. (2012). Briefly, powder was dissolved in 1.6 ml of deionized water and incubated at 100 °C for 60 min to extract carbohydrates. An aliquot of the extract was used to determine soluble sugar concentrations (i.e., glucose, fructose and sucrose) through enzymatic conversion of sucrose and fructose into glucose by invertase from *Saccharomyces cerevisiae* and phosphoglucose isomerase, respectively (I4504 and P5381, Sigma-Aldrich, Inc., Saint Louis, Missouri, USA). Total NSC concentration was

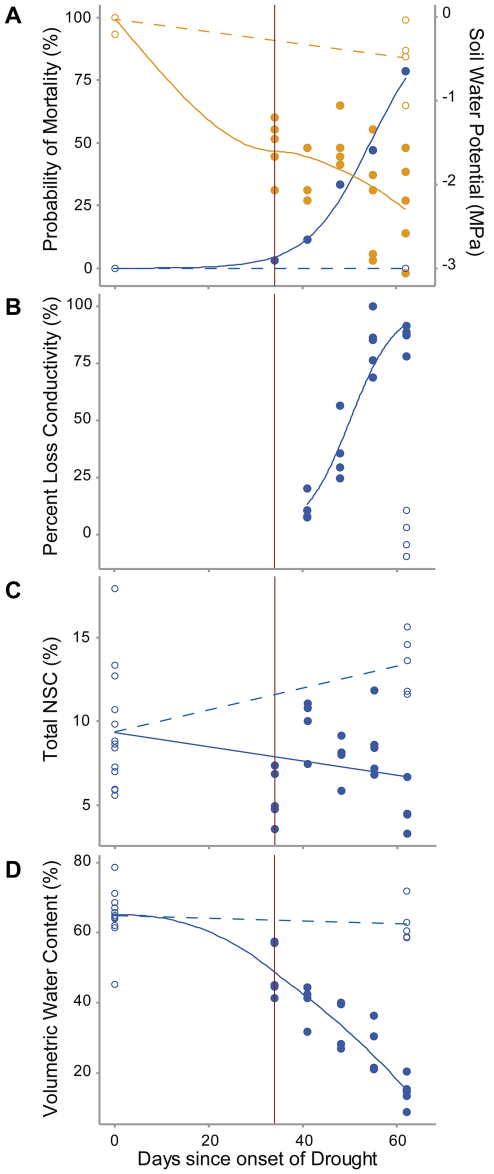

Figure 3. Dynamics of drought intensity, population-level mortality and whole-plant physiological state over time. (A) Probability of mortality (blue) increased after Day 34 of drought. Soil WPs (orange) decreased over time. (B) Significant increases of PLC (i.e., 50%) occurred several days after the first cases of mortality. (C) Non-structural carbohydrate concentrations decreased over time. (D) Volumetric water content experienced a rapid decline once mortality started. Open circles and corresponding dashed lines indicate control groups. Solid regression lines in (A), (B) and (D) are loess functions. The regression line in (C) is a linear function. These functions were chosen to best represent the natural behavior of each variable (see Table S2 available as Supplementary Data at *Tree Physiology* Online for statistics). Vertical lines indicate the initial timing of non-zero mortality risk.

obtained from another aliquot incubated in amyloglucosidase from *Aspergillus niger* (10115, Sigma-Aldrich) at 50 °C during 16 h to break down all NSC (starch included) into glucose. In both cases, the concentration of glucose was determined photometrically in a 96-well microplate reader (BioTek™ EL800, Winooski, USA) after enzymatic conversion of glucose into glucose-6-phosphate by glucose hexokinase (G3293, Sigma-Aldrich). The dehydrogenation of glucose causes an increase in optical density at 340 nm. All the NSC and soluble sugar concentrations were expressed as percentages of dry matter. Although the quantification of NSC has been proven difficult and inconsistent among laboratories, the reasonable consistency within a given laboratory allows comparisons among samples (Quentin et al. 2015). We calculated the total pool of NSCs, starch, soluble sugars and glucose or fructose in each organ by multiplying the corresponding concentration per dry mass by the dry weight. Concentrations (total NSC and each individual component) were scaled up to the whole plant by weighting by organ fraction as above.

Statistical analyses

We developed five models to evaluate trends in drought intensity, whole plant physiological status and population-level mortality over time. All models had days since the onset of drought as their predictor variable and one of the following variables as the response variable: (i) soil WP, (ii) total NSC concentration, (iii) VWC, (iv) PLC or (v) probability of mortality. Linear models were used for the first three cases given that response variables could be transformed to meet model assumptions. Generalized linear models with binomial error distribution (logit link) were used in the last two instances. Percent loss of conductivity and probability of mortality were expressed on a decimal fraction basis following requirements of models with binomial distributions.

To test whether NSC concentrations, loss of hydraulic conductivity (PLC) and VWC at each sampling time predicted population level probability of mortality, we used six linear models at the whole-plant level with the probability of mortality as the response variable. Predictor variables for each model were (i) starch and soluble sugar concentrations as separate variables within the same model to assess their separate effects, (ii) total NSC concentrations (sum of starch and soluble sugar concentrations), (iii) PLC, (iv) VWC, (v) starch and soluble sugar concentrations and PLC, and (vi) total NSC and PLC as the explanatory variables. We ran the last two models to test whether the combined predictive capacity of hydraulic and carbohydrate variables was similar to the predictive capacity of VWC alone under the hypothesis that VWC should integrate both hydraulic failure and carbon depletion (i.e., comparisons were not done to test which of these variables is the best predictor of DIM but, rather, to test whether VWC integrates PLC and NSC). Volumetric water content was log-transformed to achieve normality. We used differences in the Akaike Information Criterion (ΔAIC) and adjusted R-square values (R^2_{adj}) to rank the models in terms of simplicity and predictive power.

We used segmented linear models using the segmented function from R package *segmented* (Muggeo 2008) to explore potential threshold-type relationships between NSC, PLC or

VWC and population-level probability of mortality. Given a linear regression model, this function tries to estimate a new model with a segmented relationship (the linear function is divided into two segments, each with different slope, starting from an initial inflection point provided by the user and then identifies the actual inflection point at which the change of slope occurs). The model simultaneously optimizes the slopes and inflection point through several iterations until a local optima is achieved (Muggeo 2003). Initial inflection points were determined by visually inspecting the relationship between mortality risk and the variables of interest. We emphasize that thresholds are not meant to distinguish dead from living plants but, rather, values of a given explanatory variable above or below which the risk of mortality at the population level is no longer zero (incipient mortality risk). We used *ΔAIC* to justify the use of segmented models instead of simple linear models. Only segmented models with a *ΔAIC* equal or greater than 10 were considered to provide a better fit for the data (Burnham and Anderson 2004). In those cases, thresholds among organs and whole plant were considered significantly different when the confidence intervals of the threshold values did not overlap.

To test whether plant water content was explained by loss of hydraulic conductivity, we performed organ-level and plant-level linear models with VWC as the response variable and stem PLC, root PLC or plant PLC as predictors. We also assessed whether NSC explained VWC. Because under drought and minimal carbon supply consumption of NSC storage for metabolic demands is expected, a positive relationship between NSC and VWC could simply reflect that both variables independently responded to drought. To test whether NSC concentrations directly affected organ or whole-plant water content, we first performed two sets of organ- and plant-level linear models with VWC and NSC as the response variables and soil WP as predictor. Then, we tested whether the residuals from the relationships of VWC vs soil WP were related to those from the relationship of NSC vs soil WP, thus removing the direct effect of drought on each variable.

Results

Soil WP decreased with time in drought-stressed seedlings (Figure 3A, R^2_{adj} = 0.82, $P < 0.001$; Table S2 available as Supplementary Data at *Tree Physiology* Online). The first signs of DIM did not appear until Day 34 after the onset of drought (Figure 3A), after which the probability of mortality increased over time ($P = 0.005$; Table S2 available as Supplementary Data at *Tree Physiology* Online). Whole-plant PLC was still low at Day 41 but increased sharply over time in drought-stressed seedlings (Figure 3B, $P = 0.028$; Table S2 available as Supplementary Data at *Tree Physiology* Online) with plants reaching 50% loss of conductivity by approximately Day 50. Both whole-plant total NSC concentrations and VWC decreased over time (R^2_{adj} = 0.09, $P = 0.044$ and R^2_{adj} = 0.74, $P < 0.001$, respectively; Table S2 available as Supplementary Data at *Tree Physiology* Online). Non-structural carbohydrates declined linearly over time (Figure 3C), while VWC declined non-linearly (Figure 3D). The observed decrease in NSC was driven by a decline in starch (plant: R^2_{adj} = 0.33, $P < 0.001$; needles: R^2_{adj} = 0.18, $P = 0.005$; stem: R^2_{adj} = 0.47, $P < 0.001$; roots: R^2_{adj} = 0.48, $P < 0.001$; Figure S1 available as Supplementary Data at *Tree Physiology* Online), which offset an increase in soluble sugars (plant: R^2_{adj} = 0.62, $P < 0.001$; needles: R^2_{adj} = 0.06, $P = 0.08$; stem: R^2_{adj} = 0.51, $P < 0.001$; roots: R^2_{adj} = 0.53, $P < 0.001$; Figure S1 available as Supplementary Data at *Tree Physiology* Online).

Volumetric water content at each sampling time was negatively related to probability of mortality (R^2_{adj} = 0.90, $P < 0.001$), both at the whole-plant (Figure 4) and organ level (Figure S2 and Tables S3 and S4 available as Supplementary Data at *Tree Physiology* Online). Percent loss of conductivity and NSC were positively and negatively related, respectively, to probability of mortality (R^2_{adj} = 0.82, $P < 0.001$ and R^2_{adj} = 0.14, $P < 0.009$, respectively). However, only PLC was highly correlated with mortality based on R^2_{adj} (Figure S3 and Table S3 available as Supplementary Data at *Tree Physiology* Online). Segmented models identified thresholds for incipient mortality for VWC at VWC = 47.3 ± 7.61% (VWC value below which the risk of mortality was no longer zero and started to increase rapidly), but failed to find such thresholds for PLC and NSC (Figure S3 and Table S4 available as Supplementary Data at *Tree Physiology* Online). Although failure to detect PLC thresholds could be due to methodological issues (how PLC is estimated and missing PLC values until Day 41 of drought), results appeared robust to uncertainty in PLC estimates generated by using different sets of individuals to measure native and maximum conductivity/conductance (Methods S1 available as Supplementary Data at *Tree Physiology* Online). These results were also robust to differences in sample size and timing of data collection among explanatory variables due to missing PLC values from early stages of the drought (Methods S3 available as Supplementary Data at *Tree Physiology* Online). When VWC was assessed at the organ level, needles and roots also showed a threshold-type response (Figure S2 and Table S4 available as Supplementary Data at *Tree Physiology* Online). Thresholds in needles and roots were not significantly different despite the observed variability among organs due to differences in VWC at full turgor.

Percent loss of conductivity increased as soil WPs decreased (plant: R^2_{adj} = 0.39, $P = 0.002$; stem: R^2_{adj} = 0.39, $P = 0.002$; roots: R^2_{adj} = 0.33, $P = 0.005$), and VWC was strongly related to PLC in all organs and at the whole-plant level (plant: R^2_{adj} = 0.74, $P < 0.001$; stem: R^2_{adj} = 0.54, $P < 0.001$; roots: R^2_{adj} = 0.52, $P < 0.001$) (Figure 5; Table S5a available as Supplementary Data at *Tree Physiology* Online). Volumetric water content was also correlated with NSC depletion

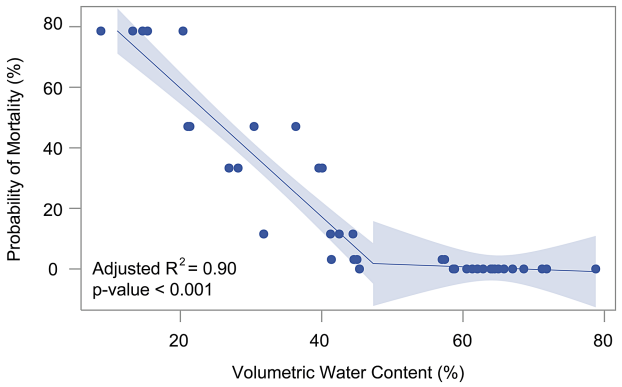

Figure 4. Whole-plant VWC predicts mortality risk and shows a threshold response (i.e., identifies a threshold of incipient DIM risk) based on segmented linear regression. Probability of mortality increases sharply after the population reaches whole plant VWC values >47.3 ± 7.61. Shaded areas represent 95% confidence intervals of the regression lines. Note that data from different time points are included.

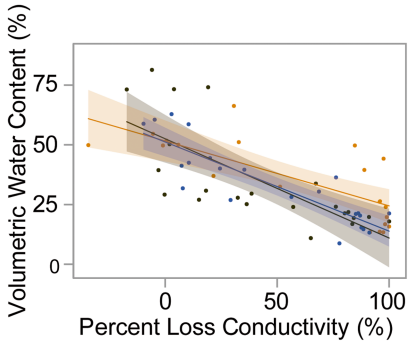

Figure 5. Whole-plant VWC decreases as water supply is lost (measured as PLC). The response is similar across all measured organs (stems: orange; roots: brown) and at the whole-plant level (blue). Shaded areas represent 95% confidence intervals of the regression lines. See Table S5a available as Supplementary Data at *Tree Physiology* Online for statistical details.

(Figure S4 available as Supplementary Data at *Tree Physiology* Online), as both decreased with drought. The residuals from the relationship of VWC vs soil WP and those from the relationship of NSC vs soil WP were positively correlated (plant: $R^2 = 0.67$, $P < 0.001$; needles: $R^2 = 0.20$, $P = 0.041$; roots: $R^2 = 0.21$, $P = 0.024$) (Figure 6D–F; Table S5a available as Supplementary Data at *Tree Physiology* Online), indicating that VWC and NSC were related independent of soil WP (see statistical analyses section for rationale behind this analysis). Contrary to expectations, however, the effect of NSC on VWC was driven by starch, not by soluble sugars (Figure 6D–F; Table S5b available as Supplementary Data at *Tree Physiology* Online) as supported by the lack of a significant relationship between sugar residuals and VWC residuals (Figure 6D–F).

Discussion

Our experimental design based on the point of no return shows that VWC identifies DIM risk, at both the whole-plant (Figure 4) and organ levels (Figure S2, and Tables S3 and S4 available as Supplementary Data at *Tree Physiology* Online). As expected, PLC also reflects mortality risk. However, in this study, PLC did not detect incipient mortality risk. Regardless of whether PLC may also be able to detect incipient mortality risk in other species or studies, the ability of VWC to predict incipient mortality risk is relevant and useful because VWC integrates both hydraulic failure and carbon depletion processes and can be measured at different scales (Martinez-Vilalta et al. 2019).

The threshold-like response of VWC (Figure 4; Figure S2 available as Supplementary Data at *Tree Physiology* Online) or other water content-related variables is expected based on physiological principles: DIM risk is low over ranges of water content sufficient to maintain turgor, but may increase substantially as water content in organs decreases below values leading to turgor loss. Although plants can recover from temporary turgor loss, continued decreases of water content below turgor loss may increase the risk of irreversible turgor loss due to cellular damage (Trueba et al. 2019). As widespread and permanent loss of turgor in living cells unavoidably leads to tissue (and eventually whole plant) death, variables related to water content have the potential to signal incipient DIM risk thresholds across species (Martinez-Vilalta et al. 2019) and assess mortality risk across communities (Hartmann et al. 2018).

In our study the relationship between PLC and probability of mortality was linear rather than showing an inflection point that distinguishes healthy from at-risk plants (Figure S3 and Table S4 available as Supplementary Data at *Tree Physiology* Online). However, in other studies, PLC has been shown to cause a threshold-like response in DIM at the individual (Brodribb and Cochard 2009, Urli et al. 2013) and population levels (Barigah et al. 2013). Although our sensitivity analyses suggest that our results are robust to missing PLC values at Days 0 and 34 and variation due to estimations of PLC based on population-level *K*max (Methods S1 and S3 available as Supplementary Data at *Tree Physiology* Online), it is important to note that PLC thresholds may be apparent at other life stages, populations or species as suggested by the results in Barigah et al. (2013). The lack of incipient PLC thresholds at the population level could also be due to greater variability in PLC thresholds among individuals within our population than for VWC thresholds. Martinez-Vilalta et al. (2019) showed that threshold-type relationships between mortality risk and physiological variables at the population level become shallower the greater the variation in threshold values among individuals. These relationships can even become linear if within-population variation is large enough. While recent evidence suggests that thresholds based on water content tend to show less variation (Trueba et al. 2019), many more assessments of both individual- and population-level mortality are needed to further test this hypothesis. Therefore, our study does

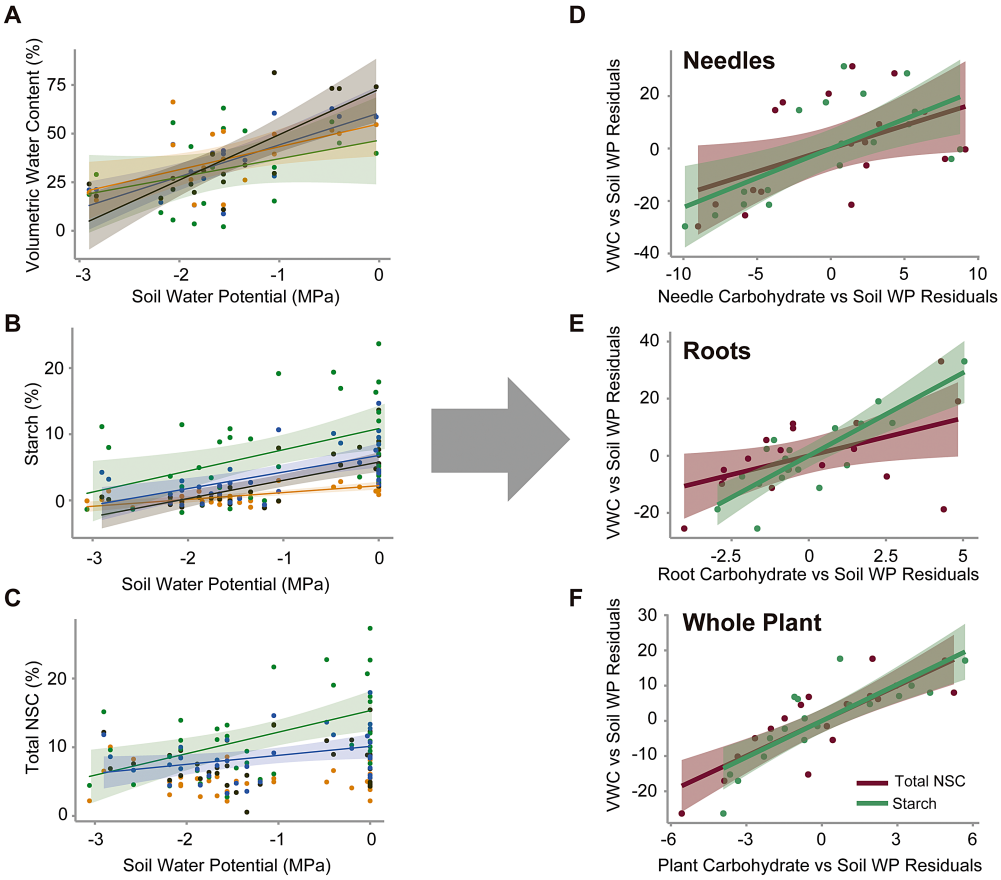

Figure 6. Water retention depends on NSC storage. The positive correlation between the residuals of the regression between plant VWC vs soil WP and those between NSC vs soil WP indicates that for a given soil WP, if NSCs were higher than expected, then VWC was also higher than expected. Left panels represent relationships between (A) VWC, (B) starch concentrations and (C) total NSC concentrations and soil WP. Colors within (A), (B) and (C) represent needles (light green), stems (orange), roots (brown) and whole plant (blue). Right panels display residuals of the relationship between VWC and soil WP as a function of residuals of the relationships between carbohydrates (NSC or starch) and soil WP in each organ. Colors within (D), (E) and (F) represent NSC (purple) and starch (dark green). Carbohydrate contents are represented as percentage of dry mass. Only significant regressions are shown and NSC components for which there was no significant relationship (glucose + fructose and sucrose) are not shown. Shaded areas are 95% confidence intervals of the regression lines. *P*-values in residual analyses ranged between <0.001 and 0.04 and adjusted R^2 values ranged between 0.20 and 0.68 (Tables S5a and S5b available as Supplementary Data at *Tree Physiology* Online).

not indicate that VWC is better than PLC at predicting DIM. Rather, in this study we demonstrate that water content, a variable that has received little focus during the past decade of DIM research, is also a useful indicator of DIM risk, and can reliably distinguish populations at no risk from those at risk of DIM (i.e., incipient mortality risk), a critical feature for monitoring purposes. Thus, our results in ponderosa pine suggest that water content variables are worth considering along other classic DIM predictors such as PLC, WP and NSC.

Our results also support that water content integrates the diverse mechanisms leading to drought mortality. When stomata close under drought, plant water content depends on loss via cuticular conductance and stomatal leakiness, along with the water supply through the vascular system (Blackman et al. 2016). Consistently, VWC was strongly related to PLC in all organs and at the whole-plant level (Figure 5; Table S5a available as Supplementary Data at *Tree Physiology* Online). Volumetric water content also decreased significantly with NSC depletion (Figure S4 available as Supplementary Data at *Tree Physiology* Online), which occurred as the drought intensified and starch concentration decreased, likely as a result of decreased supply via photosynthesis (Figure S1 available as Supplementary Data at *Tree Physiology* Online). In contrast, soluble sugars, the osmotically active component of NSC, increased during drought (Figure S1 available as Supplementary Data at *Tree Physiology* Online), a common response (Martinez-Vilalta et al. 2016). Critically, VWC residuals and NSC residuals were strongly related, indicating that NSC storage is involved directly and/or indirectly in tissue water retention (independent of direct drought effects on both variables). Contrary to expectations, however, the effect of NSC on VWC was driven by starch, not by soluble sugars (Figure 6D–F; Table S5b available as Supplementary Data at *Tree Physiology* Online). Such a response could represent conversion of starch into osmolytes other than sucrose, glucose and fructose (e.g., raffinose) that would not be detected by our methods (Lintunen et al. 2016).

Alternatively, NSC could serve as an energy source for the active accumulation of both organic and inorganic solutes (White and Broadley 2001; Plett and Møller 2010). Overall, our results at the whole-plant and organ level show that metrics of water content accurately capture the progressive dehydration leading to desiccation that occurs during the process of DIM (Tyree et al. 2003; Saiki et al. 2017). Plants regulate water content by preventing loss of hydraulic conductivity or PLC, enhancing retention (including capacitance) and reducing water loss (Meinzer et al. 2001) (Figure 1). We find that both water supply (PLC) and NSC influence VWC and that failure to maintain water content above certain thresholds increases risk of death (Figure 1).

Incorporating water content-related variables may advance our current conceptual framework for predicting DIM based on hydraulic failure and carbon starvation (Mcdowell et al. 2008): water content integrates important aspects of the two mechanisms (Figures 5 and 6) and provides a metric to which living cells respond directly (Zhu 2016; Sack et al. 2018). Consistent with recent evidence (Adams et al. 2017), our results show that hydraulic failure (i.e., water supply) has a dominant effect on DIM relative to NSC storage depletion (i.e., water retention) (Figure S3 and Table S3 available as Supplementary Data at *Tree Physiology* Online). The degree to which hydraulic failure and NSC depletion contribute to changes in plant water balance likely varies across populations, species and biomes (Anderegg 2015; Adams et al. 2017) but such variability is potentially captured by water content. Thus, water content variables may provide more consistent relationships with mortality risk across species than PLC or NSC alone because they integrate the two.

Another potential advantage of adding water content to current frameworks for assessing DIM is that it can be measured across scales ranging from organs to ecosystems via remote sensing (Saatchi and Moghaddam 2000; Ceccato et al. 2001; Ullah et al. 2014; Ma et al. 2016; Fang et al. 2017; Konings et al. 2017). In contrast, PLC is more difficult to measure at large spatial scales, and values leading to mortality are variable across organs and species (Tyree et al. 2003, Brodribb and Cochard 2009, Choat et al. 2012, Urli et al. 2013). The relationship between water content and DIM reported here is currently limited to seedlings, and experimental evidence in mature trees is still needed. However, declines in remotely sensed water content have been linked to mortality of mature trees across diverse forest types (Saatchi et al. 2013, Asner et al. 2015, Rao et al. 2019). Therefore, water content may offer potential for improved monitoring of DIM risk across scales. Our results, along with those of Saatchi et al. 2013, Asner et al. 2015 and Rao et al. 2019 are promising and warrant future experimental studies on mature trees.

The expected increase in DIM under climate change has large ecological, economic and social implications (Stocker et al. 2015). Despite intense research, our limited understanding of the interaction between hydraulic failure and carbon depletion, along with the lack of physiological indicators with incipient DIM thresholds measurable at large scales have hindered our ability to accurately model and monitor DIM risk (Hartmann et al. 2018). We provide experimental evidence that plant water content is a useful indicator of DIM risk, integrates the mechanisms of DIM at the individual level and shows an incipient DIM threshold. While our results may have important implications for large-scale monitoring of DIM risk, much research is still needed. First, we measured VWC as a potential indicator because it is most similar to the variable used in remote sensing techniques. However, anatomical differences among organs and species are likely to cause a certain degree of variability in the relationship between VWC and mortality risk for both incipient mortality threshold values and the slope of the relationship beyond such values. Plant functional-type estimates of VWC mortality thresholds and slopes may provide a way to encapsulate such variability and effectively predict DIM across species. Alternatively, measures of water content that account for the water-holding capacity of the tissue, such as the relative water content (Martínez-Vilalta et al. 2019), or that account for the capacity to recover from turgor loss (Trueba et al. 2019) may provide more consistent thresholds across species. Other critical research steps include the following: (i) to corroborate that water content variables are useful for DIM assessment in other species, (ii) to assess water content mortality thresholds and slopes in mature trees, (iii) to examine similar relationships from remotely sensed data concurrent with drought mortality data and (iv) to integrate dynamics of vegetation water content in systems with multiple species and plant growth strategies. Comparative tests of the relative performance of commonly used DIM predictors such as WP, PLC and NSC against that of water content variables across populations and species may also shed light on the physiological mechanisms of DIM and the interaction between hydraulic failure and carbon depletion. We hope our results will motivate such work.

Supplementary Data

Supplementary Data for this article are available at *Tree Physiology* online.

Acknowledgments

This work was supported by a National Science Foundation (NSF) grant to S.D., M.M. and A.S. (BCS 1461576). The authors also thank Elliott Conrad, Dylan Budke and Aurora Bayless-Edwards for their assistance in data collection; Zack Holden for his feedback on the experimental design; Dan Johnson for his advice on hydraulic methods; and

Douglas Emlen, Art Woods, Ray Callaway and Danielle Way and several anonymous reviewers for insightful comments and suggestions on early versions of this manuscript. G.S. received funding from the NSF Experimental Program to Stimulate Competitive Research (EPSCoR) Track-1 EPS-1101342 (INSTEP 3). W.R.L.A acknowledges funding from the David and Lucille Packard Foundation, NSF grants 1714972 and 1802880 and the USDA National Institute of Food and Agriculture, Agricultural and Food Research Initiative Competitive Program, Ecosystem Services and Agro-ecosystem Management via grant no. 2018-67019-27850. J.M.-V. acknowledges support from the Spanish Ministry of Economy and Competitiveness via competitive grants CGL2013-46808-R and CGL2017-89149-C2-1-R and by the ICREA Academia program.

Conflict of interest

None declared.

Authors' contributions

G.S., A.S., B.R., S.D. and M.M. designed the experiment; G.S. collected and analyzed the data with contributions from A.S., S.D., B.R., W.R.L.A. and J.M.-V.; and G.S. and A.S. wrote the manuscript with edits from B.R., S.D., M.M., W.R.L.A. and J.M.-V.

Funding

This work was supported by a National Science Foundation grant to S.D., M.M. and A.S. (BCS 1461576). G.S. received funding from the NSF Experimental Program to Stimulate Competitive Research (EPSCoR) Track-1 EPS-1101342 (INSTEP 3).

References

Adams HD, Zeppel MJB, Anderegg WRL et al. (2017) A multi-species synthesis of physiological mechanisms in drought-induced tree mortality. Nat Ecol Evol 1:1285–1291.

Allen CD, Breshears DD, McDowell NG (2015) On underestimation of global vulnerability to tree mortality and forest die-off from hotter drought in the Anthropocene. Ecosphere 6:1–55.

Anderegg WRL (2015) Spatial and temporal variation in plant hydraulic traits and their relevance for climate change impacts on vegetation. New Phytol 205:1008–1014.

Anderegg WRL, Anderegg LDL (2013) Hydraulic and carbohydrate changes in experimental drought-induced mortality of saplings in two conifer species. Tree Physiol 33:252–260.

Anderegg WRL, Berry JA, Smith DD, Sperry JS, Anderegg LDL A, Field CB (2012*a*) The roles of hydraulic and carbon stress in a widespread climate-induced forest die-off. Proc Natl Acad Sci USA 109: 233–237.

Anderegg WRL, Berry JA, Field CB (2012*b*) Linking definitions, mechanisms, and modeling of drought-induced tree death. Trends Plant Sci 17:693–700.

Anderegg WRL, Flint A, Huang C, Flint L, Berry JA, Davis FW, Sperry JS, Field CB (2015) Tree mortality predicted from drought-induced vascular damage. Nat Geosci 8:367–371.

Asner GP, Brodrick PG, Anderson CB, Vaughn N, Knapp DE, Martin RE (2015) Progressive forest canopy water loss during the 2012–2015 California drought. Proc Natl Acad Sci USA 113(2):E249–E255.

Barigah TS, Charrier O, Douris M, Bonhomme M, Herbette S, Améglio T, Fichot R, Brignolas F, Cochard H (2013) Water stress-induced xylem hydraulic failure is a causal factor of tree mortality in beech and poplar. Ann Bot 112:1431–1437.

Blackman CJ, Pfautsch S, Choat B, Delzon S, Gleason SM, Duursma RA (2016) Toward an index of desiccation time to tree mortality under drought. Plant Cell Environ 39:2342–2345.

Brodersen CR, McElrone AJ, Choat B, Matthews MA, Shackel KA (2010) The dynamics of embolism repair in xylem: in vivo visualizations using high-resolution computed tomography. Plant Physiol 154:1088–1095.

Brodribb TJ, Cochard H (2009) Hydraulic failure defines the recovery and point of death in water-stressed conifers. Plant Physiol 149:575–584.

Burnham KP, Anderson DR (2004) Multimodel inference: understanding AIC and BIC in model selection. Sociol Methods Res 33: 261–304.

Ceccato P, Flasse S, Tarantola S, Jacquemoud S, Grégoire JM (2001) Detecting vegetation leaf water content using reflectance in the optical domain. Remote Sens Environ 77:22–33.

Chaturvedi AK, Patel MK, Mishra A, Tiwari V, Jha B (2014) The SbMT-2Gene from a halophyte confers abiotic stress tolerance and modulates ROS scavenging in transgenic tobacco. PLoS One 9(10):1–12.

Choat B, Jansen S, Brodribb TJ et al. (2012) Global convergence in the vulnerability of forests to drought. Nature 491:752–755.

Cregg BM (1994) Carbon allocation, gas exchange, and needle morphology of *Pinus ponderosa* genotypes known to differ in growth and survival under imposed drought. Tree Physiol 14:883–898.

Dickman LT, Mcdowell NG, Sevanto S, Pangle RE, Pockman WT (2015) Carbohydrate dynamics and mortality in a piñon-juniper woodland under three future precipitation scenarios. Plant Cell Environ 38:729–739.

Espino S, Schenk HJ (2011) Mind the bubbles: achieving stable measurements of maximum hydraulic conductivity through woody plant samples. J Exp Bot 62:1119–1132.

Fang M, Ju W, Zhan W, Cheng T, Qiu F, Wang J (2017) A new spectral similarity water index for the estimation of leaf water content from hyperspectral data of leaves. Remote Sens Environ 196:13–27.

Fredlund DG, Xing A (1994) Equations for the soil-water characteristic curve. Can Geotech J 31:521–532.

Galiano L, Martínez-Vilalta J, Sabaté S, Lloret F (2012) Determinants of drought effects on crown condition and their relationship with depletion of carbon reserves in a Mediterranean holm oak forest. Tree Physiol 32:478–489.

Garcia-Forner N, Sala A, Biel C, Savé R, Martínez-Vilalta J (2016) Individual traits as determinants of time to death under extreme drought in *Pinus sylvestris* L. Tree Physiol 36: 1196–1209.

Guadagno CR, Ewers BE, Speckman HN, Aston TL, Huhn BJ, DeVore SB, Ladwig JT, Strawn RN, Weinig C (2017) Dead or alive? Using membrane failure and chlorophyll fluorescence to predict mortality from drought. Plant Physiol 175:223–234.

Hacke UG, Sperry JS, Ewers BE, Ellsworth DS, Schäfer KVR, Oren R (2000) Influence of soil porosity on water use in *Pinus taeda*. Oecologia 124:495–505.

Hartmann H, Moura CF, Anderegg WRL et al. (2018) Research frontiers for improving our understanding of drought-induced tree and forest mortality. New Phytol 218:15–28.

Hoch G, Popp M, Körner C (2002) Altitudinal increase of mobile carbon pools in Pinus cembra suggests sink limitation of growth at the Swiss treeline. Oikos 98:361–374.

Hoffmann WA, Marchin RM, Abit P, Lau OL (2011) Hydraulic failure and tree dieback are associated with high wood density in a temperate forest under extreme drought. Glob Chang Biol 17:2731–2742.

Hughes SW (2005) Archimedes revisited: a faster, better, cheaper method of accurately measuring the volume of small objects. Phys Educ 40:468–474.

Kolb PF, Robberecht R (1996) High temperature and drought stress effects on survival of *Pinus ponderosa* seedlings. Tree Physiol 16:665–672.

Konings AG, Piles M, Rötzer K, McColl KA, Chan SK, Entekhabi D (2016) Vegetation optical depth and scattering albedo retrieval using time series of dual-polarized L-band radiometer observations. Remote Sens Environ 172:178–189.

Konings AG, Yu Y, Xu L, Yang Y, Schimel DS, Saatchi SS (2017) Active microwave observations of diurnal and seasonal variations of canopy water content across the humid African tropical forests. Geophys Res Lett 44:2290–2299.

Kursar TA, Engelbrecht BMJ, Burke A, Tyree MT, El B, Giraldo JP (2009) Tolerance to low leaf water status of tropical tree seedlings is related to drought performance and distribution. Funct Ecol 23:93–102.

Lewis SL, Brando PM, Phillips OL, van der GMF, Nepstad D (2011) The 2010 Amazon drought. Science 331:554.

Lintunen A, Paljakka T, Jyske T et al. (2016) Osmolality and non-structural carbohydrate composition in the secondary phloem of trees across a latitudinal gradient in Europe. Front Plant Sci 7:1–15.

Ma B, Xu A, Zhang S, Wu L (2016) Retrieval of leaf water content for maize seedlings in visible near infrared and thermal infrared spectra. 2016 IEEE International Geoscience and Remote Sensing Symposium (IGARSS), Beijing 6930–6933.

Martinez-Vilalta J, Sala A, Asensio D, Galiano L, Hoch G, Palacio S, Piper FI, Lloret F (2016) Dynamics of non-structural carbohydrates in terrestrial plants: a global synthesis. Ecol Monogr 86:495–516.

Martinez-Vilalta J, Anderegg WRL, Sapes G, Sala A (2019) Greater focus on water pools may improve our ability to understand and anticipate drought-induced mortality in plants. New Phytol 223:22–32.

McDowell NG (2011) Mechanisms linking drought, hydraulics, carbon metabolism, and vegetation mortality. Plant Physiol 155:1051–1059.

McDowell N, Pockman WT, Allen CD et al. (2008) Mechanisms of plant survival and mortality during drought: why do some plants survive while others succumb to drought? New Phytol 178:719–739.

Meinzer FC, Clearwater MJ, Goldstein G (2001) Water transport in trees: current perspectives, new insights and some controversies. Environ Exp Bot 45:239–262.

Meir P, Mencuccini M, Dewar RC (2015) Drought-related tree mortality: addressing the gaps in understanding and prediction. New Phytol 207:28–33.

Mencuccini M, Minunno F, Salmon Y, Martínez-Vilalta J, Hölttä T (2015) Coordination of physiological traits involved in drought-induced mortality of woody plants. New Phytol 208:396–409.

Mirzaie M, Darvishzadeh R, Shakiba A, Matkan AA, Atzberger C, Skidmore A (2014) Comparative analysis of different uni- and multi-variate methods for estimation of vegetation water content using hyper-spectral measurements. Int J Appl Earth Obs Geoinf 26: 1–11.

Muggeo V (2003) Estimating regression models with unknown break-points. Stat Med 22:3055–3071.

Muggeo V (2008) Segmented: an R package to fit regression models with broken-line relationships. R News 8:20–25.

O'Brien MJ, Leuzinger S, Philipson CD, Tay J, Hector A (2014) Drought survival of tropical tree seedlings enhanced by non-structural carbohydrate levels. Nat Clim Chang 4:710–714.

Olesen PO (1971) Forest tree improvement Vol. 3: The water displacement method; a fast and accurate method of determining the green volume of wood samples. Akademisk Forlag, Copenhagen.

Plett DC, Møller IS (2010) Na+ transport in glycophytic plants: what we know and would like to know. Plant Cell Environ 33: 612–626.

Pratt RB, Jacobsen AL, Ramirez AR, Helms AM, Traugh CA, Tobin MF, Heffner MS, Davis SD (2014) Mortality of resprouting chaparral shrubs after a fire and during a record drought: physiological mechanisms and demographic consequences. Glob Chang Biol 20:893–907.

Quentin AG, Pinkard EA, Ryan MG et al. (2015) Non-structural carbohydrates in woody plants compared among laboratories. Tree Physiol 35:1146–1165.

Rao K, Anderegg WRL, Sala A, Martínez-Vilalta J, Konings AG (2019) Satellite-based vegetation optical depth as an indicator of drought-driven tree mortality. Remote Sens Environ 227: 125–136.

Rowland L, da ACL, Galbraith DR et al. (2015) Death from drought in tropical forests is triggered by hydraulics not carbon starvation. Nature 528:119–122.

Saatchi SS, Moghaddam M (2000) Estimation of crown and stem water content and biomass of boreal forest using polarimetric SAR imagery. IEEE Trans Geosci Remote Sens 38:697–709.

Saatchi S, Asefi-Najafabady S, Malhi YEOC, Aragão ALO, Myneni RB, Nemani R (2013) Persistent effects of a severe drought on Amazonian forest canopy. Proc Natl Acad Sci USA 110:565–570.

Sack L, John GP, Buckley TN (2018) ABA accumulation in dehydrating leaves is associated with decline in cell volume not turgor pressure. Plant Physiol 176:489–493.

Saiki ST, Ishida A, Yoshimura K, Yazaki K (2017) Physiological mechanisms of drought-induced tree die-off in relation to carbon, hydraulic and respiratory stress in a drought-tolerant woody plant. Sci Rep 2995:1–7.

Sala A, Woodruff DR, Meinzer FC (2012) Carbon dynamics in trees: feast or famine? Tree Physiol 32:764–775.

Sevanto S, McDowell NG, Dickman LT, Pangle R, Pockman WT (2014) How do trees die? A test of the hydraulic failure and carbon starvation hypotheses. Plant Cell Environ 37:153–161.

Sperry JS, Donnelly JR, Tyree MT (1988) A method for measuring hydraulic conductivity and embolism in xylem. Plant Cell Environ 11:35–40.

Stocker TF, Qin D, Plattner GK et al. (2015) Summary for policymakers. In: Climate change 2013: the physical science basis. Contribution of Working Group I to the Fifth Assessment Report of the Intergovernmental Panel on Climate Change. CEUR Workshop Proceedings 1542:33–36.

Torres-Ruiz JM, Sperry JS, Fernández JE (2012) Improving xylem hydraulic conductivity measurements by correcting the error caused by passive water uptake. Physiol Plant 146:129–135.

Torres-Ruiz JM, Jansen S, Choat B et al. (2015) Direct X-ray microtomography observation confirms the induction of embolism upon xylem cutting under tension. Plant Physiol 167:40–43.

Trifilo P, Barbera PM, Raimondo F, Nardini A, MAL G (2014) Coping with drought-induced xylem cavitation: coordination of embolism repair and ionic effects in three Mediterranean evergreens. Tree Physiol 34:109–122.

Trueba S, Pan R, Scoffoni C, John GP, Davis SD, Sack L (2019) Thresholds for leaf damage due to dehydration: declines of hydraulic

function, stomatal conductance and cellular integrity precede those for photochemistry. New Phytol 223:134–49.

Tyree MT, Sperry JS (1989) Vulnerability of xylem to cavitation and embolism. Ann Rev Plant Phys Mol Biol 40:19–38.

Tyree MT, Engelbrecht BMJ, Vargas G, Kursar TA, States U, Forest A, Box PO, Vermont MTT (2003) Desiccation tolerance of five tropical seedlings in Panama. Relationship to a field assessment of drought performance. Plant Physiol 132:1439–1447.

Ullah S, Skidmore AK, Naeem M, Schlerf M (2012) An accurate retrieval of leaf water content from mid to thermal infrared spectra using continuous wavelet analysis. Sci Total Environ 437:145–152.

Ullah S, Skidmore AK, Ramoelo A, Groen TA, Naeem M, Ali A (2014) Retrieval of leaf water content spanning the visible to thermal infrared spectra. ISPRS J Photogramm Remote Sens 93:56–64.

Urli M, Porté AJ, Cochard H, Guengant Y, Burlett R, Delzon S (2013) Xylem embolism threshold for catastrophic hydraulic failure in angiosperm trees. Tree Physiol 33:672–683.

Veysi S, Naseri AA, Hamzeh S, Bartholomeus H (2017) A satellite based crop water stress index for irrigation scheduling in sugarcane fields. Agric Water Manag 189:70–86.

Wang C-R, Yang A-F, Yue G-D, Gao Q, Yin H-Y, Zhang J-R (2008) Enhanced expression of phospholipase C 1 (ZmPLC1) improves drought tolerance in transgenic maize. Planta 227: 1127–1140.

White PJ, Broadley MR (2001) Chloride in soils and its uptake and movement within the plant: a review. Ann Bot 88:967–988.

Williams A, Allen CD, Macalady AK et al. (2013) Temperature as a potent driver of regional forest drought stress and tree mortality. Nat Clim Chang 3:292–297.

Yilmaz MT, Hunt ER, Jackson TJ (2008) Remote sensing of vegetation water content from equivalent water thickness using satellite imagery. Remote Sens Environ 112:2514–2522.

Zhu J-K (2016) Abiotic stress signaling and responses in plants. Cell 167:313–324.